Journal of Organometallic Chemistry 961 (2022) 122262

Contents lists available at ScienceDirect

Journal of Organometallic Chemistry

journal homepage: www.elsevier.com/locate/jorganchem

C – C coupling of ethyne to the carbido ligand in products from reactions with Ru$_5$(μ_5–C)(CO)$_{15}$

Richard D. Adams*, Humaiara Akter, Mark D. Smith

Department of Chemistry and Biochemistry, University of South Carolina, Columbia, SC, 29208

ARTICLE INFO

Article history:
Received 17 December 2021
Accepted 10 January 2022
Available online 13 January 2022

Keywords:
Carbido ligand
Carbido – alkyne coupling
Ruthenium
Cluster opening
Carbon chain growth
Structural analyses

ABSTRACT

The reaction of Ru$_5$(μ_5−−C)(CO)$_{15}$, **1** with C$_2$H$_2$ at 48 °C for 60 h yielded four new pentaruthenium carbonyl cluster compounds: Ru$_5$[μ_5-η^5-CC(H)C(H)C(H)C(H)](CO)$_{13}$(μ_4-η^2-HCCH), **2**; Ru$_5$[μ_4-η^5-CC(H)C(H)C(H)C(H)](CO)$_{12}$(μ_4-η^2-HCCH), **3**; Ru$_5$(CO)$_{13}$[μ_4-η^7-C(H)C(H)CC(H)C(H)C(H)C(H)], **4** and Ru$_4$(CO)$_{11}$(μ_4-η^2-HCCH)Ru(CO)$_3$(μ-η^1-η^5-C$_5$H$_4$), **5**. Compounds **2** and **3** were formed by opening of the Ru$_5$ cluster of **1**, the addition of three equivalents of C$_2$H$_2$, two of which became coupled to each other and to the carbido ligand of **1** to form bridging CC(H)C(H)C(H)C(H), pentadienyl ligands. Compounds **2** and **3** also contain a quadruply-bridging a η^2-HCCH ligand. Compound **4** contains an open Ru$_5$ cluster, in which three equivalents of C$_2$H$_2$ were coupled to each other and to the carbido ligand of **1** to form a quadruply-bridging heptadienyl η^7-C(H)C(H)CC(H)C(H)C(H)C(H) ligand. Compound **5** contains a butterfly-tetrahedral Ru$_4$ cluster with a quadruply-bridging a η^2-HCCH ligand and a Ru(CO)$_3$(μ-η^1-η^5-C$_5$H$_4$) grouping containing a metalated-cyclopentadienyl ligand that is linked to one of the wing-tip Ru atoms of the Ru$_4$ cluster. The metalated-cyclopentadienyl ligand in **5** is believed to have been formed by a cyclization of the bridging, CC(H)C(H)C(H)C(H), pentadienyl ligand in compound **2**. All new compounds were characterized by single-crystal X-ray diffraction analyses.

1. Introduction

Carbido ligands have attracted the interest of chemists ever since the reports of the first examples, Fe$_5$(μ_5−C)(CO)$_{15}$ [1] and Ru$_6$(μ_6−C)(CO)$_{17}$ [2], in polynuclear metal carbonyl cluster complexes. The fully-encapsulated, interstitial carbido ligand **A** has little potential for direct organic synthesis, but it does help to stabilize the metal clusters and allows for a variety of chemical reactions on the surface of the metal cluster [3]. It has been proposed that partially-exposed carbido ligands, such as **B** – **D**, will have some potential to engage in carbon – carbon and carbon – hydrogen bond-forming reactions with selected small molecules and hydrocarbyl ligands [4]. The μ$_4$- and μ-carbido ligands in **C** and **D** have been shown to exhibit a variety of interesting reactivities, see Schemes 1 and 2 [5,6].

Chung *et al.* have demonstrated the formation of a C – C bond between the carbido ligand and alkynes in a WOs$_3$ cluster complex [7].

Carbon atoms on metal surfaces are believed to have high reactivities and serve as intermediates involved in C – C coupling reactions [8] leading to the formation of hydrocarbon chains as found in Fischer-Tropsch Syntheses (FTS) [9]. FTS is a heterogeneous catalytic process that utilizes iron, cobalt, ruthenium or other catalysts for the conversion of CO and H$_2$ into hydrocarbons through surface polymerization reactions involving metal−carbide (M-C) [10] and metal−hydride (M-H) intermediates [11].

Adams *et al.* observed the formation of a C–C bond between a μ_5-carbido carbon and a phenyl group to yield a bridging benzylidyne ligand in a SnRu$_5$C cluster complex [12].

In more recent studies, we have obtained a variety of bridging and terminally-coordinated zwitterionic ammonio-alkenyl ligands formed in reactions of the carbido-pentaruthenium cluster complex Ru$_5$(μ_5−C)(CO)$_{15}$, **1** with ethyne (C$_2$H$_2$) in the presence of the CO activation reagent trimethylamineoxide, Me$_3$NO [13]. In an effort to study the ability of the bridging carbido ligand to engage in C – C coupling reactions further, the reactions of **1** with ethyne in the absence of Me$_3$NO were investigated. These studies have revealed reaction pathways dominated by C – C bond coupling between the carbido ligand in **1** and C$_2$H$_2$ to yield new ethyne-coupled Ru$_5$ cluster complexes containing hydrocarbon chains as bridging ligands including one product having a chain as long as seven carbon atoms. The structures, bonding and transformations of these new complexes are described in this report.

---

* Corresponding author.
E-mail address: Adamsrd@mailbox.sc.edu (R.D. Adams).

https://doi.org/10.1016/j.jorganchem.2022.122262

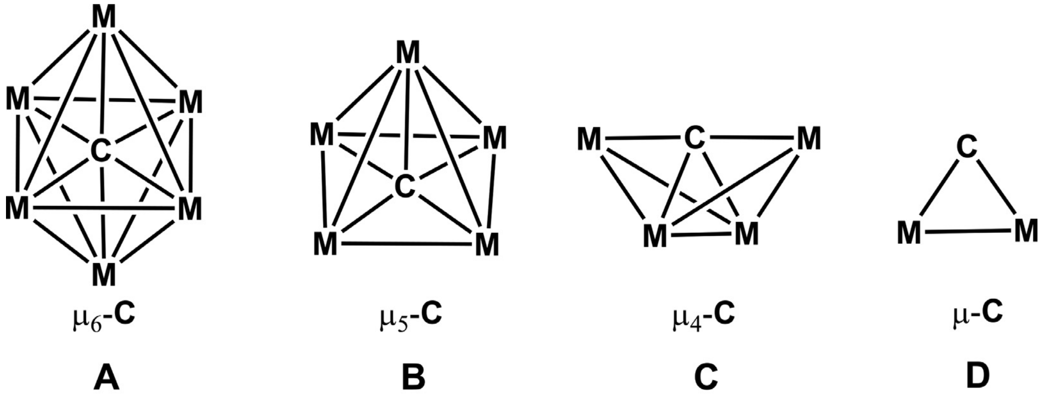

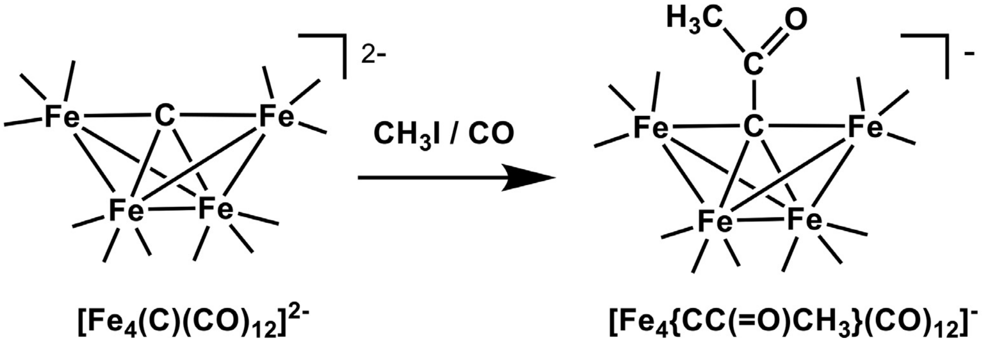

Scheme 1. .

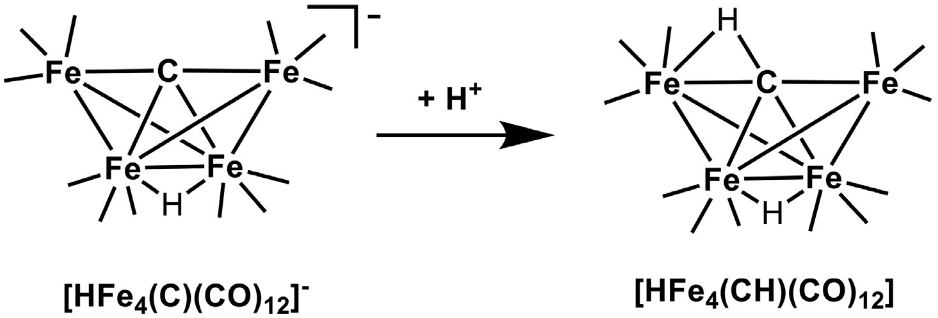

Scheme 2. .

2. Experimental section

2.1. General data

All reactions were performed under an atmosphere of nitrogen. Reagent grade solvents were dried by standard procedure and were freshly distilled prior to use. Infrared spectra were recorded on a Thermo Scientific Nicolet IS10 spectrophotometer. ^{1}H NMR spectra were recorded on Varian Mercury spectrometers operating at 300.1 MHz and 400 MHz. Mass spectrometric (MS) measurements were performed by a direct-exposure probe by using electron impact (EI) ionization. $Ru_3(CO)_{12}$ that was used to make $Ru_5(\mu_5{-}C)(CO)_{15}$, **1** was obtained from STREM and was used without further purification. Compound **1** was prepared according to a previously reported procedure [14]. Ethyne gas (HC_2H) was obtained from National Welders and was used without further purification. Carbon Monoxide (CO) was purchased from Airgas Specialty Chemicals and was used without further purification. **WARNING**: Carbon Monoxide and ethyne are hazardous gasses that should be used only in a well-ventilated fume hood. Product separations were performed by TLC in the air on Analtech 0.25 mm and 0.50 mm silica gel 60 Å F254 glass plates, and silica gel column chromatography on silica gel 60, 0.606 - 0.2 mm (70 – 230 mesh).

2.2. Reaction of $Ru_5(\mu_5{-}C)(CO)_{15}$, 1, with C_2H_2 at 48 °C

A 49.9 mg (0.053 mmol) amount of **1** was dissolved in 4 mL of CD_2Cl_2 solvent and was then transferred to three NMR tubes in equal amounts. The NMR tubes were closed with rubber septa and then sealed with parafilm. C_2H_2 gas at 1 atm bubbled through the solutions for 30 s. The tubes were sealed under an atmosphere C_2H_2. After shaking for few times tubes were heated to 48 °C in a constant temperature oil bath. The reaction progress was monitored by both ^{1}H NMR and IR spectroscopy. After purging with C_2H_2 four times and heating at 48 °C for 60 h the reaction was complete. The products were then separated by TLC by using a solvent mixture of hexane/methylene chloride to yield four bands in the order of elution: 3.7 mg of orange red $Ru_5[\mu_5\text{-}\eta^5\text{-}CC(H)C(H)C(H)C(H)](CO)_{13}(\mu_4\text{-}\eta^2\text{-}HCCH)$, **2** (7% yield), 1.0 mg of red $Ru_5[\mu_4\text{-}\eta^5\text{-}CC(H)C(H)C(H)C(H)](CO)_{12}(\mu_4\text{-}\eta^2\text{-}HCCH)$, **3** (2% yield), 0.9 mg of orange $Ru_5(CO)_{13}[\mu_4\text{-}\eta^7\text{-}C(H)C(H)CC(H)C(H)C(H)C(H)]$, **4** (2% yield), 6.0 mg of orange $Ru_4(CO)_{11}(\mu_4\text{-}\eta^2\text{-}HCCH)Ru(CO)_3(\mu\text{-}\eta^1\text{-}\eta^5\text{-}C_5H_4)$, **5** (11% yield). Spectral data for **2**: IR, ν_{CO} (cm^{-1} in hexane): 2093 (w), 2073 (vs), 2048 (s), 2028 (m), 2021 (w), 2014 (s), 2003 (w), 1984 (vw), 1969 (w). ^{1}H NMR (in acetone-d_6, δ in ppm): 9.28 (CC**H**CHCHC**H**, dd, $^3J_{H-H} = 8.0$ Hz, $^3J_{H-H} = 1.5$ Hz, 1H), 7.80 (μ_4–C**H**CH, d, $^3J_{H-H} =$ **8.0** Hz, 1H), 7.24 (μ_4–C**H**CH, d, $^3J_{H-H} = 6.6$ Hz, 1H), 5.70 (CCHC**H**C**H**CH, m, 1H), 5.34 (CCHC**H**C**H**CH, m, 1H), 4.80 (CC**H**CHCHC**H**, d, $^3J_{H-H} = 6.3$ Hz, 1H). EI/MS *m/z.* $M^+ = 959.5$. The isotope distribution pattern is consistent with the presence of five ruthenium atoms. Spectral data for **3**: IR, ν_{CO} (cm^{-1} in hexane): 2089 (w), 2080 (vw), 2059 (s), 2049 (w), 2034 (vs), 2014 (s), 2004 (w), 1983 (w), 1967 (w). ^{1}H NMR (in acetone-d_6, δ in ppm): 10.02 (μ_4–C**H**CH, d, $^3J_{H-H} = 6.0$ Hz, 1H), 9.23 (CC**H**CHCHC**H**), dd, $^3J_{H-H} = 7.5$ Hz, $^4J_{H-H} = 1.5$ Hz, 1H), 7.56 (μ_4–CHC**H**, d, $^3J_{H-H} = 6.0$ Hz, 1H), 7.24 (CC**H**CHCHC**H**), d, $^3J_{H-H} = 6.9$ Hz, 1H), 6.80 (CCHC**H**C**H**CH), dd, $^3J_{H-H} = 7.5$ Hz, $^3J_{H-H} = 6.9$ Hz, 1H), 6.48 (CCHC**H**C**H**CH**,** ddd, $^3J_{H-H} = 7.5$ Hz, $^3J_{H-H} = 6.9$ Hz, $^3J_{H-H} = 1.5$ Hz, 1H). Spectral data for **4**: IR, ν_{CO} (cm^{-1} in Hexane): 2093 (w), 2073 (vs), 2051 (vs), 2039 (w), 2031 (m), 2016 (m), 1998 (w), 1981 (w), 1945 (w). ^{1}H NMR (in CD_2Cl_2 solvent, δ in ppm): 9.89 (C**H**CHCCHCHCHCH, d, $^3J_{H-H} = 6.6$ Hz, 1H), 7.96 (CHCHCC**H**CHCHCH, d, $^3J_{H-H} = 7.8$ Hz, 1H), 6.76 (CHC**H**CCHCHCHCH, d, $^3J_{H-H} = 6.6$ Hz, 1H), 6.28 (CHCHCCHC**H**CHCH, m, 1H), 6.13 (CHCHCCHCHC**H**CH, d, $^3J_{H-H} = 7.8$ Hz, 1H), 5.88 (CHCHCCHCHCHC**H**, dd, 1H, $^3J_{H-H} = 7.8$ Hz, $^3J_{H-H} = 4.8$ Hz). Spectral data for **5**: IR, ν_{CO} (cm^{-1} in CH_2Cl_2): 2116 (w), 2086 (vw), 2069 (m), 2060 (m), 2029 (s), 2011 (vs), 1989 (w), 1970 (w). ^{1}H NMR (in acetone-d_6, δ in ppm): 9.93 (μ_4–C**H**C**H,** s, 2H), 6.26 (CC**H**CHCHC**H**, dd, $^3J_{H-H} = 1.8$ Hz, 2H), 5.91 (CCHC**H**C**H**CH, dd, $^3J_{H-H} = 1.8$ Hz, 2H).

2.3.Thermal transformation of 2 to 3 and 5 at 48 °C

A 9.1 mg (0.0095 mmol) amount of **2** was dissolved in CD_2Cl_2 solvent in an NMR tube. The NMR tube was sealed with a rubber septum and degassed under vacuum/nitrogen cycles three times. Then the tube was heated at 48 °C in a constant temperature oil bath. Reaction progress was monitored by ^{1}H NMR spectroscopy. After heating for 18 h, the solvent was removed, and the products were isolated by TLC by using a hexane/methylene chloride solvent mixture to yield in order of elution: 1.3 mg of unreacted **2**, 1.4 mg of **3** (16% yield), and 2.5 mg of **5** (27% yield).

2.4. Carbonylation of 3 at 25 °C

3.4 mg (0.0036 mmol) of **3** was dissolved in an NMR tube in 3.0 mL of CD_2Cl_2 solvent. The NMR tube was sealed with rubber septa and degassed under nitrogen three times. CO at 1 atm pressure was then purged through the solution for 30 s at room temperature. The progress of the reaction was by monitored ^{1}H NMR spectroscopy. After 2 h at room temperature, the reaction was complete. The reaction mixture was then separated by TLC plate by using a hexane/methylene chloride solvent mixture to yield in order of elution: 2.6 mg of **2** (74% yield) and 0.3 mg of **5** (8% yield).

2.5. Thermal conversion of 2 to 5 and $Ru_4(CO)_{12}(\mu_4\text{–-}C_2H_2)$, 6 at 68 °C

10.5 mg (0.011 mmol) of **2** was dissolved in 50 mL three neck flask in dry distilled hexane. The progress of the reaction was monitored by IR spectroscopy. After refluxing at 68 °C for 50 min., the solvent was removed in *vacuo*. The reaction mixture was separated on a TLC plate by using a hexane/methylene chloride mixture to yield in order of elution: 4.1 mg of the known compound $Ru_4(CO)_{12}(\mu_4\text{–}C_2H_2)$, **6** (48% yield) [15], and 0.5 mg of **5** (5% yield).

Table 1
Crystal data and data collection parameters for compounds **2** - **5**.

Compound	2	3
Empirical formula	$Ru_5O_{13}C_{20}H_6$	$Ru_5O_{12}C_{19}H_6$
Formula weight	959.60	931.59
Crystal system	Monoclinic	Triclinic
Lattice parameters		
a (Å)	11.6680(5)	9.5052(8)
b (Å)	10.2320(4)	9.9126(8)
c (Å)	20.7513(8)	14.6411(12)
α (deg)	90.00	96.529(2)
β (deg)	99.651(2)	103.350(2)
γ (deg)	90.00	117.827(2)
V ($Å^3$)	2442.37(17)	1147.01(16)
Space group	$P2_1/c$	*P*-1
Z value	4	2
ρ_{calc} (g/cm^3)	2.610	2.697
μ (Mo Kα) (mm^{-1})	3.088	3.280
Temperature (K)	100(2)	100(2)
$2\Theta_{max}$ (°)	56.71	56.756
No. Obs. ($I > 2\sigma(I)$)	5480	4955
No. parameters	368	343
Goodness of fit (GOF)	1.035	1.047
Max. shift in cycle	0.002	0.001
Residuals*: R1; wR2	0.0193/0.0426	0.0261/0.0472
Absorption correction, Coeff. Max/min	Multi-scan 0.7457/0.6476	Multi-scan 0.6205/0.5766
Largest peak in Final Diff. Map ($e^-/Å^3$)	1.127	1.317

Compound	4	5
Empirical formula	$Ru_5O_{13}C_{20}H_6$	$Ru_5O_{14}C_{21}H_6$
Formula weight	959.60	987.61
Crystal system	Triclinic	Monoclinic
Lattice parameters		
a (Å)	8.8115(4)	12.0677(5)
b (Å)	10.6704(5)	17.0832(7)
c (Å)	13.4282(6)	13.4170(6)
α (deg)	102.952(2)	90.00
β (deg)	93.294(2)	103.619(2)
γ (deg)	94.093(2)	90.00
V ($Å^3$)	1223.78(10)	2688.2(2)
Space group	*P*-1	$P2_1/n$
Z value	2	4
ρ_{calc} (g/cm^3)	2.604	2.440
μ (Mo Kα) (mm^{-1})	3.082	2.812
Temperature (K)	100(2)	100(2)
$2\Theta_{max}$ (°)	58.48	65.354
No. Obs. ($I > 2\sigma(I)$)	5885	9050
No. parameters	368	386
Goodness of fit (GOF)	1.051	1.095
Max. shift in cycle	0.001	0.002
Residuals*: R1; wR2	0.0172/0.0305	0.0169/0.0317
Absorption correction, Coeff. Max/min	Multi-scan 0.7458/0.6496	Multi-scan 0.5655/0.4066
Largest peak in Final Diff. Map ($e^-/Å^3$)	0.713	0.544

* $R1 = \Sigma_{hkl}(||F_{obs}|-|F_{calc}||)/\Sigma_{hkl}|F_{obs}|$; $wR2 = [\Sigma_{hkl}w(|F_{obs}|-|F_{calc}|)^2/\Sigma_{hkl}wF^2_{obs}]^{1/2}$, $w = 1/\sigma^2(F_{obs})$; $GOF = [\Sigma_{hkl}w(|F_{obs}|-|F_{calc}|)^2/(n_{data} - n_{vari})]^{1/2}$.

2.6. Thermal degradation of 5 with formation of 6 and $[Ru(\eta^5\text{-}C_5H_5)(CO)_2]_2$, 7

4.6 mg (0.0046 mmol) of **5** was dissolved in d_8-toluene solvent and then transferred to an NMR tube. The tube was then closed and degassed under vacuum/nitrogen addition cycles three times.

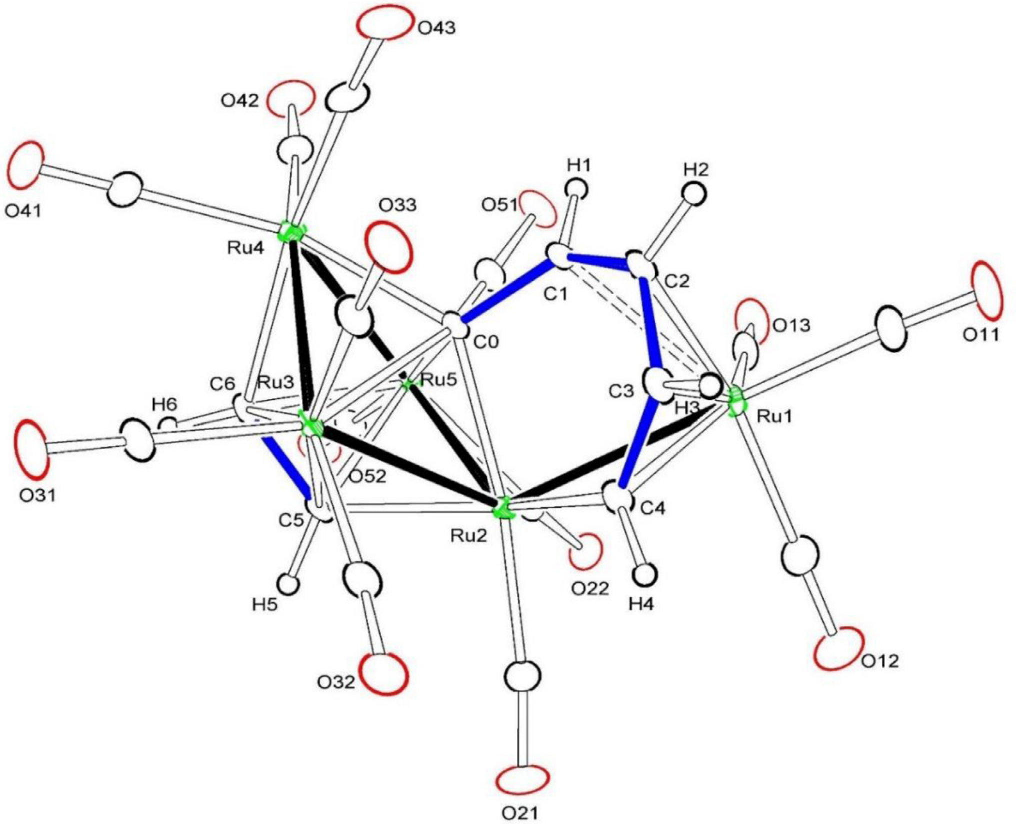

Figure 1. ORTEP diagram of the molecular structure of $Ru_5(CO)_{13}[\mu_5\text{-}\eta^5\text{-}CC(H)C(H)C(H)C(H)](\mu_4\text{-}\eta^2\text{-}HCCH)$, **2** showing 25% thermal ellipsoid probability. Selected interatomic distances (Å) are as follows: Ru1−Ru2 **=** 2.8328(3), Ru2−Ru5 = 2.6920(3), Ru2−Ru3 = 2.7121(3), Ru4−Ru5 = 2.7849(3), Ru3−Ru4 = 2.7398(3), Ru2···Ru4 = 3.904(1), Ru3···Ru5 = 3.651(1), C0−C1 = 1.444(3), C1−C2 = 1.407(4), C2−C3 = 1.438(4), C3−C4 = 1.409(4), C5−C6 = 1.416(4), Ru2−C4 = 2.050(3), Ru1−C1 = 2.499(3), Ru1−C2 = 2.227(3), Ru1−C3 = 2.205(3), Ru1−C4 = 2.191(3), Ru2−C0 = 2.099(2), Ru3−C0 = 2.324(2), Ru4−C0 = 2.144(3), Ru5−C0 = 2.284(2), Ru3−C6 = 2.290(2), Ru4−C6 = 2.117(2), Ru5−C6 = 2.304(2), Ru2−C5 = 2.152(2), Ru3−C5 = 2.244(2), Ru5−C5 = 2.278(2).

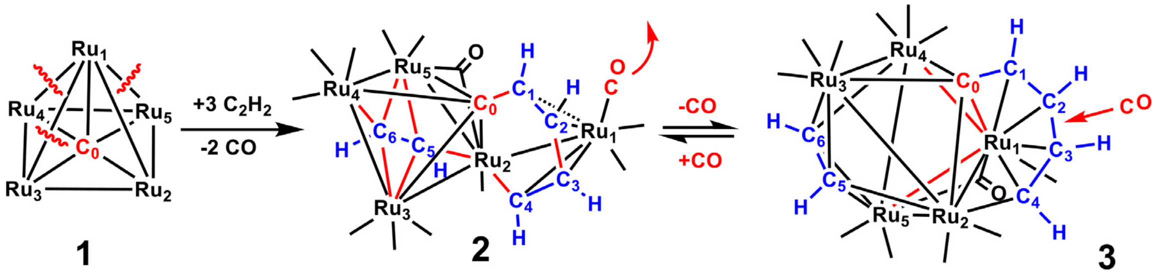

Scheme 3. A schematic for a transformation of compound **1** to **2** and **2** to **3**. Red bonds indicate where new bonds are formed. The atoms in **3** have been labeled to correspond to those in **2**.

The tube was then heated in a constant temperature oil bath at 70 °C for 6.5 days. The progress of the reaction was monitored by ^1H NMR spectroscopy. The solvent was removed in vacuo and the reaction mixture was then separated by TLC plate by using a hexane/methylene chloride/acetone solvent mixture to yield in order of elution: 1.2 mg of **6** (39% yield), and 0.6 mg of unreacted **5**. The known compound $[Ru(\eta^5\text{-}C_5H_5)(CO)_2]_2$, **7** was identified by IR, ^1H NMR spectroscopy (7.7% yield determined by NMR integration) and mass spectral analysis [16].

2.7. Crystallographic analyses

Single crystals of compounds **2** - **5** suitable for X-ray diffraction analyses were obtained by slow evaporation of solvent from solutions of the pure compounds at room temperature. Red crystals of compound **2** were obtained from a CH_2Cl_2/hexane solvent mixture. Dark red crystals of compound **3** were obtained from a CH_2Cl_2/heptane solvent mixture. Red crystals of compound **4** were obtained from a benzene/heptane solvent mixture. Red crystals of compound **5** were obtained from a benzene/heptane solvent mixture. X-ray intensity data for compounds **2** - **5** were measured by using a Bruker D8 QUEST diffractometer equipped with a PHOTON-100 CMOS area detector and an Incoatec microfocus source (Mo Kα radiation, $\lambda = 0.71073$ Å) [17]. The raw area detector data frames for compounds **2** - **5** were reduced, scaled, and corrected for absorption effects using the SAINT [17] and SADABS [18] programs. All structures were solved by using SHELXT [19]. Subsequent difference Fourier calculations and full-matrix least-squares refinement on F^2 were performed with SHELXL-2018 [18] by using OLEX2 [20]. All non-hydrogen atoms were refined with anisotropic displacement parameters.

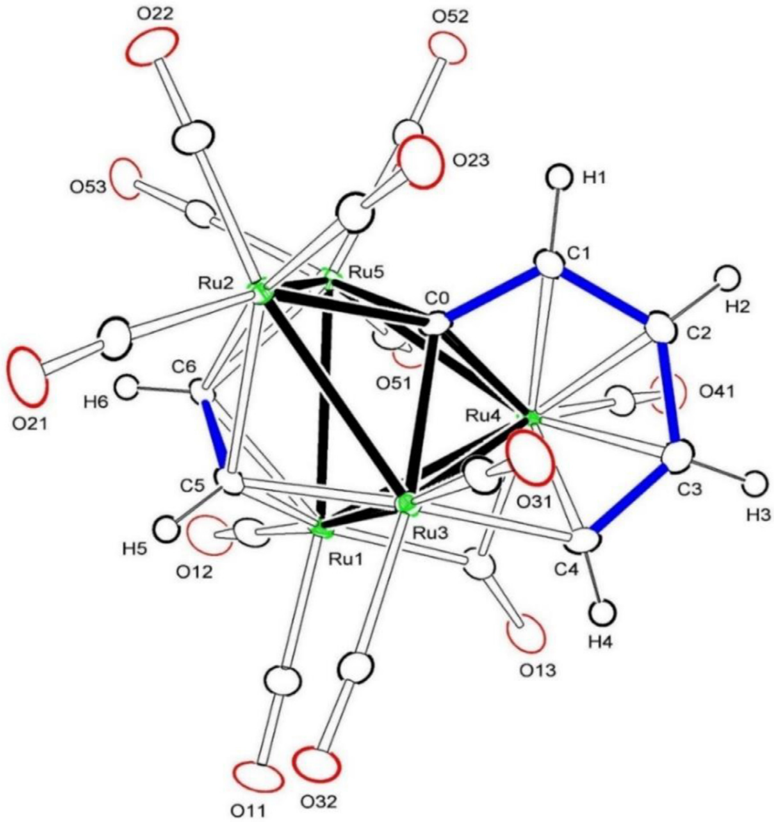

Figure 2. ORTEP diagram of the molecular structure of $Ru_5(CO)_{12}[\mu_4\text{-}\eta^5\text{-CC(H)C(H)C(H)C(H)}](\mu_4\text{-}\eta^2\text{-HCCH})$, **3** showing 35% thermal ellipsoid probability. Selected interatomic distances (Å) are as follows: Ru1−Ru3 = 2.9087(4), Ru1−Ru4 = 2.7999(4), Ru1−Ru5 = 2.8856(4), Ru2−Ru3 = 2.7920(4), Ru2−Ru5 = 2.8486(4), Ru3−Ru4 = 2.8106(4), Ru4−Ru5 = 2.8658(4), Ru1···Ru2 = 3.952(1), Ru3···Ru5 = 3.727(1), C0−C1 = 1.426(5), C1−C2 = 1.418(5), C2−C3 = 1.432(5), C3−C4 = 1.410(5), C5−C6 = 1.420(5), Ru3−C4 = 2.060(4), Ru4−C1 = 2.297(3), Ru4−C2 = 2.249(4), Ru4−C3 = 2.208(4), Ru4−C4 = 2.176(4), Ru2−C0 = 2.119(3), Ru3−C0 = 2.114(3), Ru4−C0 = 2.159(3), Ru5−C0 = 2.300(3), Ru1−C5 = 2.273(3), Ru2−C5 = 2.281(3), Ru3−C5 = 2.112(4), Ru1−C6 = 2.286(3), Ru2−C6 = 2.283(3), Ru5−C6 = 2.134(3).

Compound **2** crystallized in the monoclinic system. The pattern of systematic absences in the intensity data indicated the space group $P2_1/c$, which was confirmed by structure solution. The asymmetric unit consists of one complete molecule. All hydrogen atoms were located in difference Fourier maps and were refined freely. Compound **3** crystallized in the triclinic system. The space group *P*-1 was selected and subsequently confirmed by the successful solution and refinement of the structure. The asymmetric unit consists of one complete molecule. The six unique hydrogen atoms were located in difference Fourier maps. Their coordinates were refined freely with displacement parameters treated as $U\text{iso(H)} = 1.2U\text{eq(C)}$. Compound **4** crystallized in the triclinic system. The space group *P*-1 was selected and confirmed by the successful solution and refinement of the structure. The asymmetric unit consists of one complete molecule. The six unique hydrogen atoms bonded to the carbon atoms were located in difference Fourier maps and were refined freely. Compound **5** crystallized in the monoclinic system. The pattern of systematic absences in the intensity data was uniquely consistent with the space group $P2_1/n$, which was confirmed by the successful solution and refinement of the structure. The asymmetric unit consists of one complete molecule. The hydrogen atoms bonded to carbon atoms were located in difference Fourier maps and were refined freely. Crystal data, data collection parameters, and refinement results for each analysis are listed in Table 1.

3. Results

The reaction of **1** with C_2H_2 at 48 °C for 60 h in CD_2Cl_2 solvent yielded four new pentaruthenium carbonyl cluster compounds. They were separated by TLC and in order of elution, they were identified as $Ru_5[\mu_5\text{-}\eta^5\text{-CC(H)C(H)C(H)C(H)}](CO)_{13}(\mu_4\text{-}\eta^2\text{-HCCH})$, **2** (7% yield), $Ru_5[\mu_4\text{-}\eta^5\text{-CC(H)C(H)C(H)C(H)}](CO)_{12}(\mu_4\text{-}\eta^2\text{-HCCH})$, **3** (2% yield), $Ru_5(CO)_{13}[\mu_4\text{-}\eta^7\text{-C(H)C(H)CC(H)C(H)C(H)C(H)}]$, **4** (2% yield), and $Ru_4(CO)_{11}(\mu_4\text{-}\eta^2\text{-HCCH})Ru(CO)_3(\mu\text{-}\eta^1\text{-}\eta^5\text{-}C_5H_4)$, **5** (11% yield).

Compound **2** was characterized by IR and ^1H NMR spectroscopy, mass spectrometry, and single-crystal X-ray diffraction analysis. An ORTEP diagram of the molecular structure of **2** is shown in Fig. 1. Compound **2** was formed by the loss of two CO ligands from **1** and the addition of three equivalents of C_2H_2. Two of the C_2H_2 molecules have been coupled to each other and to the carbido ligand to form a quintuply-bridging CC(H)C(H)C(H)C(H) metallapentadienyl ligand. The third C_2H_2 group is an isolated quadruply-bridging di-σ + di-π; $\mu_4\text{-}\eta^2$-HCCH ligand. The $\mu_4\text{-}\eta^2$-HCCH ligand bridges the four metal atoms Ru(2), Ru(3), Ru(4), and Ru(5) that are arranged in the form a distorted square. The Ru – Ru bonds, Ru2−Ru5 = 2.6920(3) Å, Ru2−Ru3 = 2.7121(3) Å, Ru4−Ru5 = 2.7849(3) Å, Ru3−Ru4 = 2.7398(3) Å are similar in length to those in the butterfly cluster complex $Ru_4(CO)_{12}(\mu_4\text{–}C_2H_2)$, **6**, 2.7946(8) Å, 2.769(3) Å and 2.725(3) Å [15], but there is no significant Ru – Ru bonding across diagonals of the Ru_4 "square" in **2**: Ru2···Ru4 = 3.904(1) Å, Ru3···Ru5 = 3.651(1) Å, as there is in **6**. There is a bridging CO ligand, C(22) – O(22), across the shortest Ru – Ru bond, Ru(2) – Ru(5). Atom Ru(1) is the "spike" bonded to atom Ru(2) of the Ru_4 group, Ru1−Ru2 = 2.8328(3) Å. The C5−C6 distance, 1.416(4) Å, is similar to the C – C distance found in complex **6**, C – C = 1.472(9) Å [15]. The considerable lengthening of the C – C bond of the C_2H_2 ligand is due to the

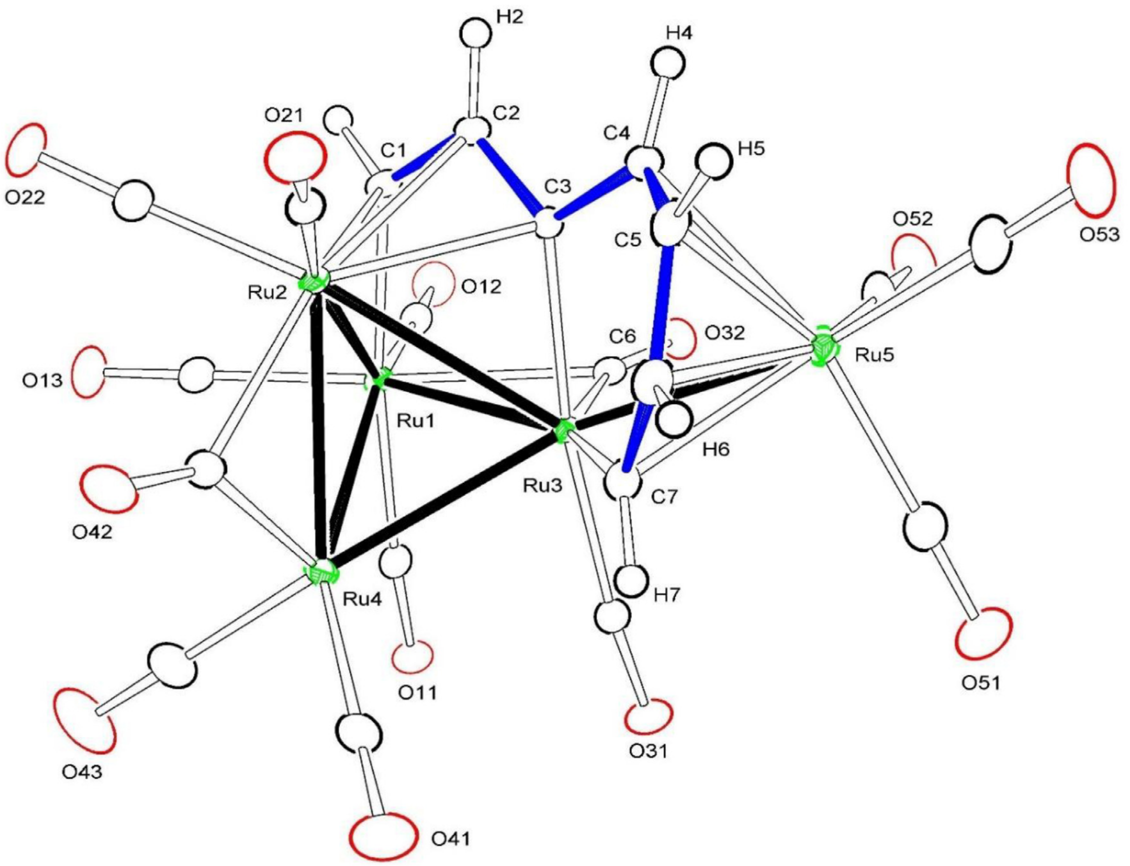

Figure 3. ORTEP diagram of the molecular structure of $Ru_5(CO)_{13}[\mu_4\text{-}\eta^7\text{-}C(H)C(H)CC(H)C(H)C(H)C(H)]$, **4** showing 40% thermal ellipsoid probability. Selected interatomic bond distances (Å) are as follows: Ru1−Ru2 = 2.8253(2), Ru1−Ru3 = 2.8146(2), Ru1−Ru4 = 2.8161(2), Ru2−Ru3 = 2.8330(2), Ru2−Ru4 = 2.8299(2), Ru3−Ru4 = 2.7213(2), Ru3−Ru5 = 2.8655(2), C1−C2 = 1.411(3), C2−C3 = 1.427(3), C3−C4 = 1.457(3), C4−C5 = 1.410(3), C5−C6 = 1.419(3), C6−C7 = 1.416(3), Ru1−C1 = 2.080(2), Ru2−C1 = 2.226(2), Ru2−C2 = 2.2725(19), Ru2−C3 = 2.2606(18), Ru3−C3 = 2.0259(19), Ru3−C7 = 2.029(2), Ru5−C4 = 2.344(2), Ru5−C5 = 2.218(2), Ru5−C6 = 2.237(2), Ru5−C7 = 2.254(2).

use of both C – C π – bonds for bonding to the metal atoms combined with the associated π – back-bonding to the alkyne from the four metal atoms [15].

The CC(H)C(H)C(H)C(H) ligand bridges all five metal atoms. The former carbido ligand, C(0), is coordinated to the Ru_4 square: Ru2−C0 = 2.099(2) Å, Ru3−C0 = 2.324(2) Å, Ru4−C0 = 2.144(3) Å and Ru5−C0 = 2.284(2) Å and coupled to the C_4H_4 chain at C(1). The C_4H_4-chain is π-bonded to the spike, Ru1: Ru1−C1 = 2.499(3) Å, Ru1−C2 = 2.227(3) Å, Ru1−C3 = 2.205(3) Å, Ru1−C4 = 2.191(3) Å. The Ru1−C1 distance is notably longer than the three other Ru(1) – C distances and C(4) bridges the Ru(1) and Ru(2) metal – metal bond, Ru2−C4 = 2.050(3) Å. The C0 – C1 and C2 – C3 bond distances in the CC(H)C(H)C(H)C(H) ligand are 1.444(3) Å and 1.438(4) Å, respectively, and are longer than the bond distances, C1 – C2 = 1.407(4) Å and C2 – C4 = 1.409(4) Å which may contain some C – C multiple bond character.

The ^{1}H NMR spectrum of compound **2** exhibits a pair of doublets at low field, $\delta = 9.28$ and 7.80, $^3J_{H-H} = 8.0$ Hz, which have similar chemical shifts to the quadruply-bridging ethyne ligand in **6**, $\delta = 10.01$ [15]. These doublets are assigned due to the inequivalent hydrogen atoms on the carbon atoms C(6) and C(5) in **2**. Resonances at $\delta = 7.24$ and 4.80 are assigned to the hydrogen atoms on C(4), $^3J_{H-H} = 6.6$ Hz and C(1), $^3J_{H-H} = 6.3$ Hz, respectively. The multiplets at $\delta = 5.70$ and 5.34 are assigned to the hydrogen atoms on C(2)/C(3) and C(3)/C(2).

One can view compound **2** as a Ru_4C_3, *closo*–pentagonal bipyramid with Ru(3) and Ru(5) at the apices and C(0), Ru(2), C(5), C(6), and Ru(4) in the equatorial positions and a Ru-spike, Ru(1) attached to Ru(2). According to the rules of the Polyhedral Skeletal Electron Pair theory (PSEP), this *closo*–pentagonal bipyramid should contain 70 electrons and the Ru spike should contribute an additional 16 electrons to the valence shell [21] to give a total of 86 expected, cluster valence electrons CVE. This is in complete agreement with the structural formula for **2**, $Ru_5 = 40\ e^- + 13$ COs $= 26\ e^- + 3$ C $= 12\ e^- +$ 2H $= 2\ e^- +$ one bridging π-C_4H_4 group $= 6\ e^-$, which adds up to 86 CVE [21].

To form the arrangement of metal atoms observed in **2** from **1**, the metal – metal bonds between Ru1 – Ru3, Ru1 – Ru4, Ru1 – Ru5 must be cleaved in the parent cluster **1**, although other possible mechanisms are possible. Two CO ligands are eliminated and three equivalents of C_2H_2 are added. Two of the acetylenes couple and bridge the remaining Ru(1) – Ru(2) bond and one end of that C_4H_4 chain forms a bond to the carbido carbon atom C(0) to form the μ_5–CC(H)C(H)C(H)C(H) ligand, see Scheme 3. A third acetylene was added to the bottom of the Ru(2), Ru(3), Ru(4), Ru(5) square base of **1** to become the quadruply-bridging C_2H_2 ligand.

Compound **3** was characterized by IR and ^{1}H NMR spectroscopies, and a single-crystal X-ray diffraction analysis. An ORTEP diagram of the molecular structure of **3** is shown in Fig. 2. Compound **3** was formed by a loss of one CO ligand presumably from the Ru spike, Ru(1), in **2**.

That atom, labelled Ru(4) in **3**, formed two new Ru – Ru bonds, one to Ru(1) and another to Ru(5), Ru1−Ru4 = 2.7999(4) Å and Ru4−Ru5 = 2.8658(4) Å, while retaining its original bond, Ru3−Ru4 = 2.8106(4) Å, see Fig. 2.

Compound **3** contains a di-σ + di-π; μ_4-η^2-HCCH ligand bridging a folded rectangle of four ruthenium atoms Ru(1), Ru(3), Ru(2) and Ru(5) similar to that found in **2**. The C(5)–C(6) dis-

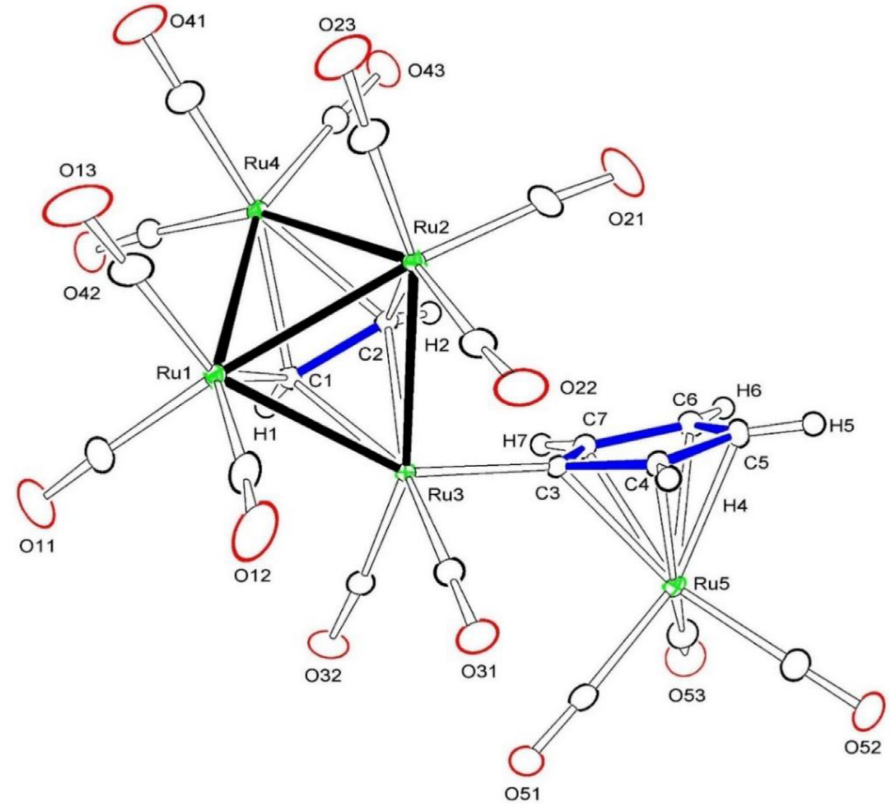

Figure 4. ORTEP diagram of the molecular structure of Ru$_4$(CO)$_{11}$((μ_4-η^2-HCCH)Ru(CO)$_3$(μ-η^1-η^5-C$_5$H$_4$), **5** showing 40% thermal ellipsoid probability. Selected interatomic bond distances (Å) are as follows: Ru1–Ru2 = 2.81061(18), Ru1–Ru3 = 2.78310(17), Ru1–Ru4 = 2.75114(19), Ru2–Ru3 = 2.77635(18), Ru2–Ru4 = 2.75564(17), C1–C2 = 1.4511(19), Ru1–C1 = 2.1087(14), Ru3–C1 = 2.1878(13), Ru4–C1 = 2.1841(13), Ru2–C2 = 2.0984(14), Ru3–C2 = 2.1984(13), Ru4–C2 = 2.1824(13), Ru3–C3 = 2.0670(13), C3–C4 = 1.4437(19), C4–C5 = 1.434(2), C5–C6 = 1.413(2), C6–C7 = 1.441(2), C7–C3 = 1.437(2), Ru5–C3 = 2.3181(13), Ru5–C4 = 2.2289(14), Ru5–C5 = 2.2310(15), Ru5–C6 = 2.2187(15), Ru5–C7 = 2.2190(14).

tance of 1.420(5) Å is similar to that in **2**. Compound **3** also contains quadruply-bridging [μ_4–CC(H)C(H)C(H)C(H)], metalla-penta-1,3-dienyl ligand, formed by the coupling of two ethyne molecules and formation of a bond to the carbido carbon C(0) of **2** that bridges the four Ru atoms, Ru(2), Ru(3), Ru(4) and Ru(5): Ru2–C0 = 2.119(3) Å, Ru3–C0 = 2.114(3) Å, Ru4–C0 = 2.159(3) Å, Ru5–C0 = 2.300(3) Å, see Scheme 3. This ligand is alsoπ-bonded to Ru(4) by the four carbon atoms C(1) through C(4); Ru4–C1 = 2.297(3) Å, Ru4–C2 = 2.249(4) Å, Ru4–C3 = 2.208(4) Å, Ru4–C4 = 2.176(4) Å and C(4) is also bonded to Ru(3), Ru3–C4 = 2.060(4) Å, to form a bridge across the Ru(3) – Ru(4) bond. The C0 – C1 and C2 – C3 bond distances, 1.426(5) Å and 1.432(5) Å, are slightly longer than the other C – C distances, C1 – C2 = 1.418(4) Å and C2 – C4 = 1.410(4) Å in the C$_5$ chain. There is a bridging carbonyl ligand C(13)-O(13) spanning the metal-metal bond between atoms Ru1 - Ru4.

The ^{1}H NMR spectrum of compound **3** shows a pair of doublets at $\delta = 10.02$ and 7.56, $^3J_{H-H} = 6.0$ Hz, that is similar to those of the hydrogen on atoms on C6 and C5 in **2** and are accordingly assigned to the ethyne hydrogen on atoms on C6 and C5 in **3**. The resonances at $\delta = 9.23$ and 6.48, $^3J_{H-H} = 7.5$ Hz are assigned due to the hydrogen atoms on C4 and C1, respectively. There is also a small coupling at the $\delta = 9.23$ resonance, $^4J_{H-H} = 1.5$ Hz due to the long-range coupling between H2 and H4. Doublets of doublets at $\delta = 6.80$ and 6.48, $^3J_{H-H} = 7.5$ Hz, $^3J_{H-H} = 6.9$ Hz, are assigned due to the hydrogen atoms on C3 and C2, respectively.

Compound **3** contains only twelve CO ligands and it can also be formed in 16% yield together with **5** in 27% yield by loss of one CO ligand in a separate reaction by heating **2** to 48 °C for 18 h. Interestingly, compound **3** will add one CO ligand at room temperature to regenerate **2** in 74% yield, see Scheme 3.

By using the formula 18x – 2y, $x = 5$, the number of metal atoms and $y = 7$, the number of metal – metal bonds, it can be shown that with a total 76 valence electrons, all the metal atoms in **3** formally have 18 electron configurations [22]. Alternatively, the Ru$_5$C$_3$ portion of the compound **3** can be viewed as *closo*–dodecahedron consisting of the five ruthenium atoms and the three carbon atoms C(0), C(5), and C(6). In this case, the cluster achieves a total cluster valence electron count of 84 electrons which is in accord with the formulation of Polyhedral Skeletal Electron Pair Theory [21].

Compound **4** was characterized by IR, ^{1}H NMR spectroscopy, and by a single-crystal X-ray diffraction analysis. An ORTEP diagram of the molecular structure of **4** is shown in Fig. 3.

Compound **4** contains five ruthenium atoms in the form of a tetrahedral cluster of four metal atoms Ru(1), Ru(2), Ru(3), and Ru(4) with one additional Ru atom as a “spike” grouping on Ru(3) of the tetrahedral group. The bond length between Ru3 – Ru5 is 2.8655(2) Å and is slightly longer than all the other Ru – Ru bond distances, 2.7213(2) Å - 2.8330(2) Å, in the tetrahedral core (find the individual Ru – Ru distances in the caption in Fig. 3). There is a seven-carbon hydrocarbyl chain, C(1) – C(7), that bridges four of the metal atoms and is coordinated to the four metal atoms by all seven carbon atoms, μ_4-η^7-C(H)C(H)CC(H)C(H)C(H)C(H). Atom C(3) has no hydrogen atoms and it is coordinated as a bridge to two Ru atoms, Ru(2) and Ru(3), Ru2–C3 = 2.2606(18) Å, Ru3–C3 = 2.0259(19) Å. The C - C bonds, C2–C3 = 1.427(3) Å and C3–C4 = 1.457(3)

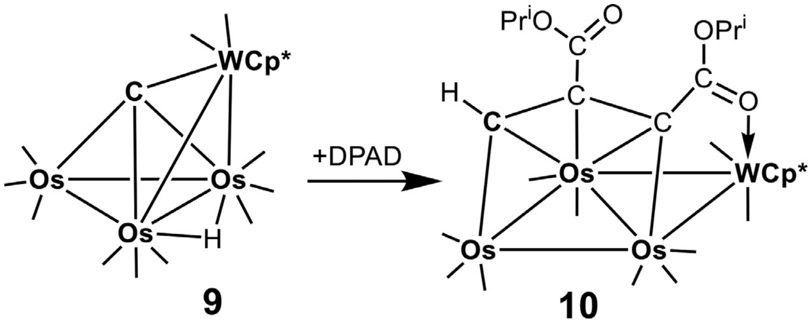

Scheme 4. A schematic of the addition and coupling of **DPAD** to carbido ligand in compound **9**.

Å, are slightly longer than the others, C1−C2 = 1.411(3) Å, C4−C5 = 1.410(3) Å, C5−C6 = 1.419(3) Å and C6−C7 = 1.416(3) Å. The latter may contain some C - C multiple bond character. Atom C(1) bridges Ru(1) and Ru(2), Ru1−C1 = 2.080(2) Å and Ru2−C1 = 2.226(2) Å, and C(7) bridges Ru(3) and Ru(5), Ru3−C7 = 2.029(2) Å and Ru5−C7 = 2.254(2) Å. Carbon atoms C(1) – C(3) are π-bonded to Ru(2), Ru2−C1 = 2.226(2), Ru2−C2 = 2.2725(19), Ru2−C3 = 2.2606(18), and atoms C(4) – C(7) are π-bonded to Ru(5), Ru5−C4 = 2.344(2) Å, Ru5−C5 = 2.218(2) Å, Ru5−C6 = 2.237(2) Å, Ru5−C7 = 2.254(2) Å.

The ^{1}H NMR spectrum of compound **4** in CD_2Cl_2 shows six resonances for the μ_4-η^7-C_7H_6 chain. A pair of doublets at $\delta = 9.89$ and 6.76 are assigned to the hydrogen atoms on atoms C1 and C2, $^3J_{H-H} = 6.6$ Hz, respectively. The resonances at $\delta = 7.96$ and 5.88 are assigned to the hydrogen atoms on C4 and C5, respectively, with $^3J_{H-H} = 7.8$ Hz. Two multiplets at $\delta = 6.28$ and 6.13 are assigned to the hydrogen atoms on C6 and C7, respectively.

It appears that C(3) is the original “carbido” terminus of a [CC(H)C(H)C(H)C(H)] ligand such as found in compounds **2** and **3** that has simply added another C_2H_2 group. Indeed, compounds **2** and **3** both contain a C_2H_2 ligand and could be precursors to **4**. However, all of our efforts to convert compounds **2** and **3** into **4** have been unsuccessful. It possible that the μ_4-C_2H_2 ligands in compounds **2** and **3** are simply too strongly coordinated to the four metal atoms in those molecules to shift to form a C – C bond to the bridging [CC(H)C(H)C(H)C(H)] ligands under mild conditions. Compound **4** contains a total of 76 cluster valence electrons which is in accord with an electron-precise metal cluster of five transition metal atoms (n) having seven metal – metal bonds (m), according to the formula 18x – 2y [22], (i.e. all metal atoms obey the Effective Atomic Number Rule).

Compound **5** was characterized by IR, ^{1}H NMR spectroscopy, and single-crystal X-ray diffraction analyses. An ORTEP diagram of the molecular structure of **5** is shown in Fig. 4.

Compound **5** contains five ruthenium atoms: four are arranged in the form a butterfly cluster having a quadruply-bridging η^2-HCCH ligand while the fifth metal atom, Ru(5), is in a $Ru(CO)_3(\mu$-η^1-η^5-$C_5H_4)$ group ligated to the Ru_4 cluster at Ru(3) via the C(3)→Ru(3) donor bond, Ru(3) – C(3) = 2.0670(13) Å, from a metalated-cyclopentadienyl ligand (C_5H_4) which is π -coordinated to Ru(5). It is presumed that the metalated-cyclopentadienyl ring, C(3) – C(7), was formed by a cyclization of the C0 – C4 chain ligand by a reductive-elimination of C0 and C4 from Ru2 in **2** which could leave the metalated-cyclopentadienyl ligand (C_5H_4) σ - bonded to Ru(3), and π-coordinated to Ru(5) in **5**, see Fig. 4. Cyclization of other alkynes by metals have also been shown to yield cyclopentadienyl ring complexes [23].

Compound **5** was also obtained together with compound **6** in 5% and 48% yields, respectively, by heating **2** to 68 °C for 50 min in hexane solvent. The bridging ethyne ligand, C(1) – C(2), is coordinated to Ru(1), Ru(3), Ru(2), and Ru(4) in the di-σ + di-π; μ_4-η^2- coordination mode, and the C(1)–C(2) bond distance equals 1.4511(19) Å. The C – C bond is oriented parallel to the hinge bond Ru(1) – Ru(2) in the Ru_4 cluster. Similarly coordinated ethyne ligands have been observed in other butterfly tetranuclear metal cluster compounds including compounds **2** and **3** [15].

The ^{1}H NMR spectrum of compound **5** shows three resonances. There is a singlet at $\delta = 9.93$ due to the two hydrogen atoms on the μ_4-ethyne ligand, and a pair of overlapping doublet of doublets at $\delta = 6.26$ and 5.91, $^3J_{H-H} = 1.8$ Hz due to the four hydrogens on the metalated η^5-C_5H_4 ligand which is coordinated to Ru(5).

The Ru_4C_2 portion of compound **5** can be viewed as *closo*–octahedron with Ru(3) and Ru(4) at two apices and Ru(1), Ru(2), C(2), and C(1) in equatorial positions. Hence, for six a skeletal electron pair (SEP) count, the Ru_4 cluster contains the expected 66 valence electron count [21] as observed, while Ru(5) has an 18 electron configuration.

When compound **5** was heated under nitrogen to 70 °C in toluene solvent for 6.5 days, it was converted to the known compounds: $Ru_4(CO)_{12}(\mu_4$–$C_2H_2)$, **6** (39% yield) [15], and $[Ru(\eta^5$-$C_5H_5)(CO)_2]_2$, **7** (7.7% yield) [16]. The formation of compound **7** was confirmed by IR and ^{1}H NMR spectroscopy, and mass spectrometry. The formation of **6** can be understood simply by the replacement of the $Ru(CO)_3(C_5H_4)$ group in **5** by a CO ligand; the CO ligand was most likely derived by a transfer from the $Ru(CO)_3(C_5H_4)$ group which was eliminated. Compound **7** must be derived by the combination of two $Ru(CO)_2(C_5H_4)$ fragments with the acquisition of a hydrogen atom by each C_5H_4 group. The source of this hydrogen atom was not confirmed.

4. Discussion

In 1997, Chi and coworkers investigated the reaction of **1** with dimethylacetylene dicarboxylate, $(MeO_2C)C_2(CO_2Me)$, **DMAD** in the presence of Me_3NO and obtained the DMAD adduct $Ru_5(\mu_5$–$C)(CO)_{15}(\mu$-η^2-$(MeO_2C)C = C(CO_2Me)]$, **8** formed by the insertion of DMAD into one of the apical-basal metal – metal bonds of **1** [24].

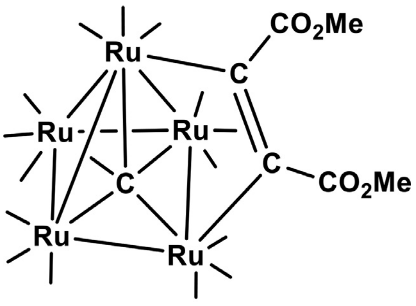

8

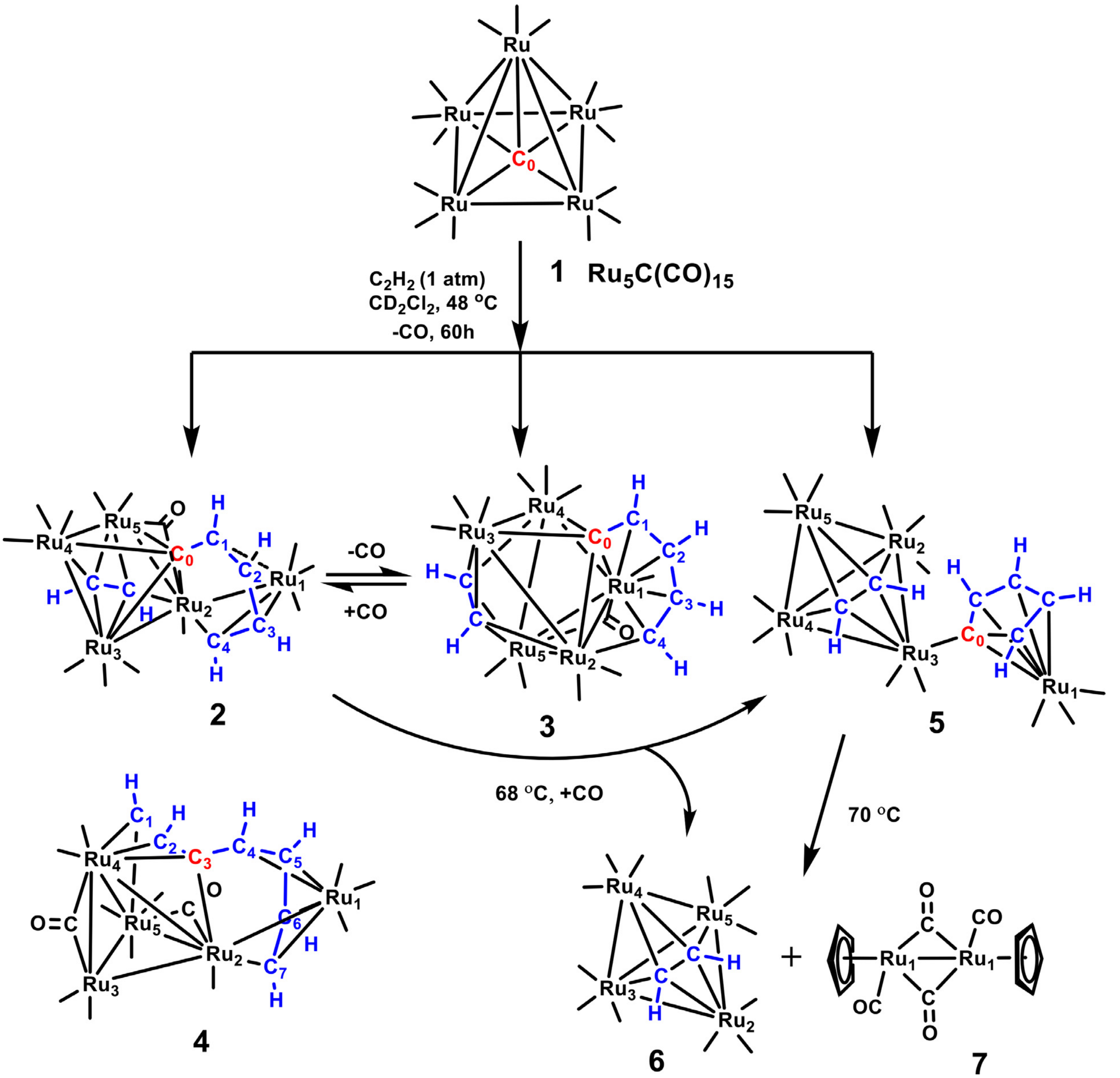

Scheme 5. A schematic of the products obtained from the reaction of **1** with ethyne (C_2H_2). Terminally coordinated CO ligands are represented only as lines from the Ru atoms.

Later they investigated the reaction of $(Cp^*)WOs_3(\mu_4{-}C)(\mu{-}H)(CO)_{11}$, **9** with di-isopropylcarboxylate acetylene, $(i{-}PrO_2C)C{\equiv}C(CO_2{-}i{-}Pr)$, **DPAD**, that yielded the complex $(Cp^*)WOs_3(CO)_{10}[\mu_4{-}HC_3(CO_2{-}i{-}Pr)_2]$, **10** containing the quadruply-bridging $[\mu_4{-}HC_3(CO_2{-}i{-}Pr)_2]$ ligand formed by opening of the cluster and C – C coupling of the DPAD molecule to the quadruply-bridging carbido ligand in **9** combined together with a transfer of the hydrido ligand to the carbido ligand, see Scheme 4[7a].

In the present work, it was found that the Ru_5 cluster compound **1** is opened by a combination of CO eliminations and multiple additions with C_2H_2 which involve C – C bond formations including coupling to the original carbido ligand of **1**. A summary of these studies is shown schematically in Scheme 5, Scheme 5 contains a new atom numbering Scheme. The reaction of **1** with C_2H_2 yielded four new ethyne containing cluster compounds.

Compound **2** has a tetranuclear Ru_4 core where an ethyne ligand is coordinated to four of the metal atoms, Ru(2), Ru(3), Ru(4), and Ru(5), in a μ_4-η^2– fashion. There is a μ_5-η^5-metalla-penta-1,3-dienyl ligand, CC(H)C(H)C(H)C(H), that was formed by the coupling of two additional C_2H_2 molecules to each other and to the carbido carbon derived from **1**. The C(H)C(H)C(H)C(H) chain in **2** bridges the Ru(1) - Ru(2) bond in a η^4:η^1 fashion. When heated to 48 °C for 18 h, compound **2** was converted to compound **3** in 16% yield and **5** in 27% yield. Compound **3** was formed by elimination of CO and the formation of two new metal – metal bonds between Ru(1) and Ru(4), and Ru(1) and Ru(5), and a switch in the bonding of C(0) from Ru(5) to Ru(1), see Scheme 5.

Compound **5** is formed concurrently by the addition of one CO molecule to **2** at Ru(2) that results in the cleavage of the metal – metal bond between Ru(1) and Ru(2). At the same time, the μ_5-η^5-metalla-penta-1,3-dienyl ligand, CC(H)C(H)C(H)C(H), that bridges the Ru(1) - Ru(2) bond in **2** is cyclized to form a metalated η^5-cyclopentadienyl ligand that is then π-coordinated to Ru(1) and σ–bonded to Ru(3), see above.

The addition of CO to compound **3** at 25 °C yielded compound **2** (yield 74%) together with a trace of **5** (yield 8%). It can be concluded that **2** is the key intermediate en route to **5** from **3**. Finally, compound **5** was converted into **6** and **7** by heating to 68 °C for 6.5 days, see Results section above for details.

5. Conclusion

These studies have shown that ethyne (HC≡CH) readily engages in multiple additions to compound **1** that lead to opening of its square-pyramidal cluster by cleavage of metal – metal bonds. The formation of C – C bonds between molecules of ethyne and the carbido ligand in **1** to yield products containing bridging ligands with C_5- and C_7- chains was also observed. In one case, compound **5**, a C_5-chain was cyclized to yield a bridging metalated-cyclopentadienyl ligand.

The coupling of alkynes to the carbido ligand observed for **1** could serve as models for carbon-chain growth processes involving reactions of carbido ligands on the surfaces of extended metal structures and heterogeneous catalysts, such as those found in catalytic Fischer-Tropsch systems [8,9].

Declaration of Competing Interest

Acknowledgement

This research was supported by grant 1764192 from the U. S. National Science Foundation.

Supplementary materials

Supplementary material associated with this article can be found, in the online version, at doi:10.1016/j.jorganchem.2022.122262.

References

[1] E.H. Braye, L.F. Dahl, W. Hübel, D.L. Wampler, The preparation, properties and structure of the iron carbonyl carbide $Fe_5(CO)_{15}C$, J. Am. Chem. Soc. 84 (1962) 4633–4639.

[2] (a) A. Sirigu, M. Bianchi, E. Benedetti, The Crystal Structure of $Ru_6C(CO)_{17}$, Chem. Commun. (1969) 596; (b) C.R. Eady, B.F.G. Johnson, J. Lewis, The Chemistry of Polynuclear Compounds. Part XXV1. Products of the Pyrolysis of Dodecacarbonyl-*triangulo*-triruthenium and -triosmium, J. Chem. Soc., Dalton Trans (1975) 2606–2611.

[3] (a)A. Reinholdt, J. Bendix, Transition Metal Carbide Complexes, *Chem Rev.* (2021) ASAP, https://doi.org/10.1021/acs.chemrev.1c00404;; (b) S. Takemoto, H. Matsuzaka, Recent advances in the chemistry of ruthenium carbido complexes, Coord. Chem. Rev. 256 (2012) 574–588; (c) J.S. Bradley, The Chemistry of Carbidocarbonyl Clusters, Adv. Organomet. Chem. 22 (1983) 1–58; (d) J.S. Bradley, Carbidocarbonyl clusters of iron, Phil. Trans. R. Soc. Lond. A 308 (1982) 103–113.

[4] (a) E.L. Muetterties, J. Stein, Mechanistic Features of Catalytic Carbon Monoxide Hydrogenation Reactions, Chem. Rev. 79 (1979) 479–490; (b) M. Tachikawa, E.L. Muetterties, Metal Carbide Clusters, Prog. Inorg. Chem. 28 (1981) 203–238; (c) J.H. Davis, M.A. Beno, J.M. Williams, J. Zimmie, M. Tachikawa, E.L. Muetterties, Structure and chemistry of a metal cluster with a four-coordinate carbide carbon atom, Proc. Nat Acad. Sci. USA 78 (1981) 668–671; (d) M. Tachikawa, R.L. Geerts, E.L. Muetterties, Metal Carbide Clusters. Synthesis Systematics for Heteronuclear Species, J. Organomet. Chem 213 (1981) 11–24.

[5] (a) J. Ohata, A. Teramoto, H. Fujita, S. Takemoto, H. Matsuzaka, Linear Hydrocarbon Chain Growth from a Molecular Diruthenium Carbide Platform, J. Am. Chem. Soc. 143 (2021) 16105–16112; (b) J.S. Bradley, S. Harris, J.M. Newsam, E.W. Hill, S. Leta, M.A. Modrick, Syntheses and Molecular and Electronic Structures of the μ_4-Methylidyne Clusters $[Fe_4(CO)_{12}C\text{-}C(O)OCH_3]^-$ and $[Fe_4(CO)_{12}C\text{-}C(CH)_3]^-$: an Analysis of Steric and Bonding Effects, *Organometallics* 6 (1987) 2060–2069.

[6] M. Tachikawa, E.L. Muetterties, Metal Clusters. 25. A uniquely bonded C-H group and reactivity of a low-coordinate carbidic carbon atom, J. Am. Chem. Soc. 102 (1980) 4541–4542.

[7] (a) C. Chung, W.-C. Tseng, Y. Chi, S.-M. Peng, G.H. Lee, Reactivity of the Tetrametallic Carbido Cluster $(C_5Me_5)WOs_3(\mu_4\text{-}C)(\mu\text{-}H)(CO)_{11}$ with Alkyne: Isomerization of an Allyl Fragment on a Tetrametallic Cluster Framework and Ring-Methyl Activation in the C_5Me_5 Ligand, *Organometallics* 17 (1998) 2207–2214; (b) Y. Chi, C. Chung, W.-C. Tseng, Y.-C. Chou, S.-M. Peng, G.-H. Lee, Alkyne–carbide coupling on WOs_3 cluster framework; synthesis and X-ray structure of $(C_5Me_5)WOs_3[\mu_4\text{-}C)(\mu\text{-}CHCHR)(CO)_{10}$ and $(C_5Me_5)WOs_3[\mu_3\text{-}CCR(CH_2)](CO)_{10}$, $R=CH_2Ph$, J. Organomet. Chem. 574 (1999) 294–301.

[8] (a) P.M. Maitlis, V. Zanotti, The role of electrophilic species in the Fischer–Tropsch reaction, Chem. Commun. (2009) 1619–1634; (b) P.M. Maitlis, R. Quyoum, H.C. Long, M.L.. T.urner, Towards a chemical understanding of the Fischer-Tropsch reaction: alkene formation, Applied Catalysis A: General 186 (1999) 363–374; (c) Z.-P. Liu, P. Hu, A New Insight into Fischer-Tropsch Synthesis, J. Am. Chem. Soc. 124 (2002) 11568–11569; (d) Y. Jiao, H. Ma, H. Wang, Y.-W. Li, X.-D. Wen, H. Jiao, Interactive network of the dehydrogenation of alkanes, alkenes and alkynes – surface carbon hydrogenative coupling on Ru(111), Catal. Sci. Technol. 11 (2021) 191–210; (e) J.M.H. Lo, T. Ziegler, Theoretical Studies of the Formation and Reactivity of C2 Hydrocarbon Species on the Fe(100) Surface, J. Phys. Chem. C 111 (2007) 13149–13162; (f) T. Li, X. Wen, Y.-W. Li, H. Jiao, Mechanisms of CO Activation, Surface Oxygen Removal, Surface Carbon Hydrogenation, and C−C Coupling on the Stepped Fe(710) Surface from Computation, J. Phys. Chem. C 122 (2018) 15505–15519; (g) D.-B. Cao, Y.-W. Li, J. Wang, H. Jiao, Adsorption and Reaction of Surface Carbon Species on Fe_5C_2 (001), J. Phys. Chem. C 112 (2008) 14883–14890.

[9] (a) I.A.W. Filot, R.A. van Santen, E.J.M. Hensen, Quantum chemistry of the Fischer–Tropsch reaction catalysed by a stepped ruthenium surface, Catal. Sci. Technol. 4 (2014) 3129–3140; (b) H. Schulz, Short history and present trends of Fischer-Tropsch synthesis, Applied Catalysis A: General 186 (1999) 3–12; (c) C.K. Rofer-DePoorter, A Comprehensive Mechanism for the Fischer-Tropsch Synthesis, Chem. Rev. 81 (1981) 447–474; (d) R.C. Brady III, R. Pettit, On the Mechanism of the Fischer-Tropsch Reaction. The Chain Propagation Step, J. Am. Chem. Soc. 103 (1981) 1287–1289; (e) F. Fischer, H. Tropsch, The Synthesis of Petroleum at Atmospheric Pressures from Gasification Products of Coal, Brennstoff-Chem 7 (1926) 97–104; (f) F.H. Pichler, Twenty-five Years of Synthesis of Gasoline by Catalytic Conversion of Carbon Monoxide and Hydrogen, Adv. Catal. 4 (1952) 271–340; (g) P. Biloen, J.N. Helle, W.M.H. Sachtler, Incorporation of surface carbon into hydrocarbons during Fischer-Tropsch synthesis: mechanistic implications, J. Catal. 58 (1979) 95–107; (h) D.-B. Cao, Y.-W. Li, J. Wang, H. Jiao, Chain growth mechanism of Fischer–Tropsch synthesis on Fe_5C_2 (001), J. Molecular Catal. A: Chem. 346 (2011) 55–69; (i) T. Li, X. Wen, Y.-W. Li, H. Jiao, Mechanistic Insight into CO Activation, methanation and C-C formation from coverage dependent CO hydrogenation on Fe(100), Surf. Sci. 689 (2019) 121456.

[10] (a) Q.Y. Liu, C. Shang, Z.P. Liu, In Situ Active Site for CO Activation in Fe-Catalyzed Fischer−Tropsch Synthesis from Machine Learning, J. Am. Chem. Soc. 143 (2021) 11109–11120; (b) M.O. Ozbek, J.W. Niemantsverdriet, Elementary reactions of CO and H_2 on C-terminated ε-Fe 5 C 2 (0 0 1) surfaces, J. Catal. 317 (2014) 158–166; (c) Y. He, P. Zhao, J. Yin, W. Guo, Y. Yang, Y.-W. Li, C.-F. Huo, X.-D. Wen, CO Direct versus H-Assisted Dissociation on Hydrogen Coadsorbed Σ-Fe_5C_2 Fischer−Tropsch Catalysts, J. Phys. Chem. C 122 (2018) 20907–20917; (d) J. Cheng, P. Hu, P. Ellis, S. French, G. Kelly, C.M. Lok, Density Functional Theory Study of Iron and Cobalt Carbides for Fischer−Tropsch Synthesis, J. Phys. Chem. C 114 (2010) 1085–1093; (e) J.M. Gracia, F.F. Prinsloo, J.W. Niemantsverdriet, Mars-van Krevelen-like Mechanism of CO Hydrogenation on an Iron Carbide, Surface. Catal. Lett. 133 (2009) 257–261; (f) Q. Zhang, J. Kang, Y. Wang, Development of Novel Catalysts for Fischer–Tropsch Synthesis: tuning the Product Selectivity, *ChemCatChem* 2 (2010) 1030–1058.

[11] P.M. Maitlis, Fischer–Tropsch, organometallics, and other friends, J. Organomet. Chem. 689 (2004) 4366–4374.

[12] R.D. Adams, B. Captain, W. Fu, M.D. Smith, High Nuclearity Ruthenium-Tin Clusters from the Reactions of Triphenylstannane with Pentaruthenium Carbonyl Carbido Cluster Complexes, Inorg. Chem. 41 (2002) 5593–5601.

[13] R.D. Adams, H. Akter, M. Kaushal, M.D. Smith, J.D. Tedder, Synthesis, Structures, and Transformations of Bridging and Terminally-Coordinated Trimethylammonioalkenyl Ligands in Zwitterionic Pentaruthenium Carbido Carbonyl Complexes, Inorg. Chem. 60 (2021) 3781–3793.

[14] B.F.G. Johnson, J. Lewis, J.N. Nicholls, J. Puga, P.R. Raithby, M. Rosales, M. McPartlin, W. Clegg, The synthesis of $[Ru_5C(CO)_{15}]$ by the carbonylation of $[Ru_6\ C(CO)_{17}]$ and the reactions of the pentanuclear cluster with a variety of small molecules: the *X*-ray structure analyses of $[Ru_5C(CO)_{15}]$, $[Ru_5C(CO)_{15}(MeCN)]$, $[Ru_5C(CO)_{14}(PPh_3)]$, $[Ru_5C(CO)_{13}(PPh_3)_2]$, and $[Ru_5(\mu\text{-}H)_2C(CO)_{12}\{Ph_2P(CH_2)_2PPh_2\}]$, J. Chem. Soc. Dalton Trans. (1983) 277–290.

[15] M.I. Bruce, B.W. Skelton, A.H. White, N.N. Zaitseva, Reactions of $Ru_3(CO)_{10}(NCMe)_2$ with ethyne: molecular structures of some prototypical cluster complexes, J. Chem. Soc., Dalton Trans. (1999) 1445–1453.

[16] H.B. Abrahamson, M.C. Palazzotto, C.L. Reichel, M.S. Wrighton, Photochemistry and electronic structure of bis(dicarbonyl(η^5-cyclopentadienyl)ruthenium) and its iron analog, J. Am. Chem. Soc. 101 (1979) 4123–4127.

[17] APEX3 Version 2016.5-0 and SAINT Version 8.37A. Bruker AXS, Inc. Madison, WI, USA.

[18] L. Krause, R. Herbst-Irmer, G.M. Sheldrick, D. Stalke, SADABS Version 2016/2, J. Appl. Cryst. 48 (2015) 3–10.

[19] (a) SHELXT: Sheldrick, G.M., Acta Cryst A71 (2015) 3–8; (b) SHELXL: Sheldrick, G.M., Acta Cryst C71 (2015) 3–8.

[20] O.V. Dolomanov, L.J. Bourhis, R.J. Gildea, J.A.K. Howard, H. Puschmann, OLEX2: a complete structure solution, refinement and analysis program, J. Appl. Cryst. 42 (2009) 339–341.

[21] (a) D.P.M. Mingos, Acc. Chem. Res. 17 (1984) 311–319; (b)D.P.M. Mingos, A.S. May, in *The Chemistry of Metal Cluster Complexes*. D. F. Shriver, H. D. Kaesz, R. D. Adams, VCH Publishers, New York, 1990, Ch. 2..

[22] P. Atkins, T. Overton, J. Rourke, M. Weller, F. Armstrong, M. Hagerman, in *Shriver & Atkins' Inorganic Chemistry*, Fifth Edition, W. H. Freeman and Co., New York, 2010, Sec 22.20, pp 564–568.

[23] (a) A.V. Kolos, Y.V. Nelyubina, B. Sundararaju, D.S. Perekalin, Synthesis of Overloaded Cyclopentadienyl Rhodium(III) Complexes via Cyclotetramerization of tert-Butylacetylene, *Organometallics* (2021) ASAP, doi:10.1021/acs.organomet.1c00403; (b) H. Komatsu, Y. Suzuki, H. Yamazaki, Unprecedented Rhodium–Mediated Tetramerization of Bulky Terminal Alkynes Leading to Hydropentalenylrhodium Complexes, Chem. Lett. 30 (2001) 998–999; (c) G. Kiefer, B. Dutta, E. Solari, R. Scopelliti, K. Severin, $RhCl_3$-Mediated Coupling Reactions of tert-Butyl Acetylene, Z. Anorg. Allg. Chem. 638 (2012) 1114–1118.

[24] C.-J. Way, Y. Chi, I.J. Mavunkal, S.-L. Wang, F.-L. Liao, S.-M. Peng, G.-H. Lee, New Electron Deficient Alkene and Alkyne Derivatives of $Ru_5(\mu_5\text{-}C)(CO)_{15}$: the Syntheses and Crystal Structure Analyses of $Ru_5(\mu_5\text{-}C)(CO)_{13}[C_2H_2(CO_2Me)_2]$ and $Ru_5(\mu_5\text{-}C)(CO)_{15}[C_2(CO_2Me)_2]$, J. Cluster Sci. 8 (1997) 87–100.